Photoemission and x-ray-absorption study of boron carbide and its surface thermal stability

I. Jiménez,* D. G. J. Sutherland, T. van Buuren, J. A. Carlisle, and L. J. Terminello
Lawrence Livermore National Laboratory, Livermore, California 94551

F. J. Himpsel
Department of Physics, University of Wisconsin-Madison, Madison, Wisconsin 53706
(Received 12 December 1997)

We present a photoemission and x-ray-absorption study on boron carbide which identifies the spectroscopic features of this material, discussing them in connection with current structural models. A study on the surface thermal stability is also performed, revealing that despite the high melting point of boron carbide ($\sim$2600 K), significant surface modifications occur in the material at about 1800 K. At this temperature the surface becomes covered with a graphite layer formed from bulk segregation of carbon, leaving boron-rich boron carbide buried beneath the graphitic surface. [S0163-1829(98)02520-X]

I. INTRODUCTION

Boron carbide is a solid whose structure is based on boron icosahedra and linear C-B-C chain building blocks.[1,2] Although the stoichiometric compound is nominally B_4C, the boron to carbon ratio can vary over a broad range by partial substitution of B by C atoms both in the C-B-C chains and in the icosahedra. This rather complex bonding structure gives the material a manifold of thermomechanical properties (low density, refractory, hard) that make it interesting for many applications as a replacement for metals, as high-temperature coatings, or as a constituent of composite ceramics.[3–5] From an electronic structure point of view, boron carbide is a semiconductor with a gap dependent on the boron to carbon stoichiometry that can be modified continuously from $\sim$0.8 eV (carbon rich) to $\sim$2 eV (boron rich),[6] and appears as a good candidate for high-temperature microelectronic devices.[7] From a fundamental standpoint, neither the atomic and electronic structures nor the electronic transport mechanisms are fully understood.[8,9] Also, there is a lack of information concerning the surface composition, structure, and properties of this material. In particular, very little has been published on surface cleaning procedures, reconstructions in single crystals, or surface stoichiometry modifications.

The use of boron carbide with other materials presents many interesting surface and interface aspects. The formation of composite ceramics based on boron carbide involves interface reactions between metals, oxides, and borides, the stability of the material being a major question.[10] Another area of interest arises from the technological problem of conditioning the graphite walls of fusion nuclear reactors by boron deposition. The neutron-absorbing boron coating lowers significantly the chemical erosion by reducing the interaction of hydrogen and oxygen ions with the carbon wall. Most of the published results concern the thickness of the boron layer attained, the location in depth of the boron atoms, and the resistance of this layer to the plasma-surface interaction.[11–13] However, the stoichiometry and structure of the boron carbide coating have largely been ignored. The interest of boron carbide as a semiconductor for high-temperature applications poses the typical interface problems of microelectronic structures, such as the electronic structure and chemical details of metal/semiconductor and insulator/semiconductor junctions.

In this work we study the photoemission and photoabsorption spectral features of boron carbide in relationship to compositional and structural changes at the surface during annealing. The aim of the study is to understand the atomic and electronic structure of this compound, information that would be useful in the characterization of boron carbide thin films, coatings, and composites. A discussion of the spectral features in terms of a simple picture of hybridization of the boron and carbon atoms is presented.

II. EXPERIMENT

We have studied by photoemission and x-ray absorption the changes that take place near the surface of a polycrystalline B_4C sample obtained from a commercial sputtering target, when heated in vacuum to temperatures up to 2100 K. The sample was cleaved in air and immediately inserted into an ultrahigh-vacuum chamber; therefore, some surface contamination is expected. To remove the contaminants we have chosen to anneal the samples in vacuum, avoiding ion sputtering cleaning procedures. Ion sputtering is not a well-suited procedure to clean the surfaces of carbon-rich solids, since it results in the formation of an amorphous graphitic layer.[14,15] In particular, to obtain clean diamond surfaces they are polished in air with an abrasive powder followed by annealing in vacuum,[16] and graphite surfaces are cleaved with an adhesive tape or annealed in vacuum to very high temperature, but never ion sputtered.[17] The B_4C samples were heated by direct flow of current, the temperature being controlled with an optical pyrometer previously calibrated. The temperature was homogeneous along the sample to within 50 K.

A set of reference samples was measured under the same conditions for direct comparison. Photoemission and photoabsorption spectra were obtained from highly oriented pyrolitic graphite (HOPG) and a diamond single-crystal (111) oriented, providing a reference for the carbon spectra. Clean

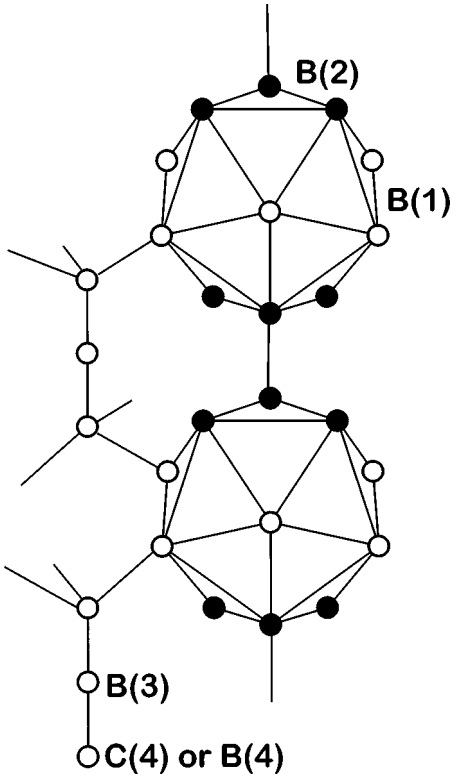

FIG. 1. Boron carbide structure.

surfaces of graphite and diamond were obtained as described above. Photoabsorption references for B($1s$) were obtained from amorphous boron, hexagonal BN (h-BN), and cubic BN (c-BN) powders epoxied to tantalum sheets.

Surface-sensitive structural information was obtained by photoemission, by monitoring B($1s$), C($1s$), and valence band photoelectrons with kinetic energies between 100 and 150 eV, which correspond to mean electron escape depths under 10 Å. Core level photoabsorption measured in the total electron yield mode probes the surface character of a material, but is not restricted to the very top atomic layers since most of the measured signal is due to low-kinetic-energy secondary electrons that have been excited deeper in the solid. Typical values of the electron escape depth in this case range from 50 to 100 Å.[18] The photoabsorption measurements were performed at the bending magnet beam line 8.2 of the Stanford Synchrotron Radiation Laboratory (SLAC), and the photoemission data were collected at the undulator beam line 8.0 of the Advanced Light Source (LBNL), both equipped with spherical grating monochromators.

III. STRUCTURAL MODELS AND BONDING ENVIRONMENTS IN BORON CARBIDE

Since photoemission and photoabsorption are both techniques sensitive to the bonding of the atoms, structural information can be obtained if the spectral features can be directly related to the different bonding environments of boron and carbon atoms in the material. Let us first consider the different bonding configurations and review existing models that have been proposed.

Figure 1 sketches the structure of boron carbide. The forming units are boron icosahedra, located at the vertices of the rhombohedral crystallographic unit cell, and three-atom linear chains located in the main diagonal that, in principle, should have the composition CCC to account for a B_4C stoichiometry. However, the structure is not so simple because of mixing of boron and carbon atoms both in the chains and icosahedra. This mixing explains the B_xC system being homogeneous within the range $4<x<11$. X-ray diffraction cannot distinguish between boron and carbon atoms due to their similar scattering factors, and the first structural studies proposed a simple B_{12}-CCC structure for B_4C.[19] Other techniques like infrared and Raman spectroscopy,[20,21] nuclear magnetic resonance,[22] and electron spin resonance[23] have provided support for the following structural model. Near the carbon-rich limit, i.e., 20 at. % carbon and B_4C stoichiometry, the solid is composed of $B_{11}C$ icosahedra and CBC chains. As the composition becomes more boron rich, CBB chains replace the CBC ones. With further carbon reduction the $B_{11}C$ icosahedra are replaced by B_{12} units. Some authors propose a first replacement of the CBC chains by CBB chains until the $B_{13}C_2$ stoichiometry is attained with a well-defined $B_{11}C$-CBB structure, followed by the change of atoms in the icosahedra.[24] Other authors propose the coexistance along the whole homogeneity range of $B_{11}C$, B_{12}, CBC, and CBB units, and the absence of the other types of linear chains, i.e., CCC, BBB, and BCB.[25]

Independent of the details of the structure, there are some general results concerning the bonding environment. In the icosahedra there are six atoms, labeled B(1), along the equator of the icosahedron, each forming five intraicosahedral bonds and one intericosahedral bond to a terminal atom in the linear chain. There are also six atoms of type B(2) forming three-atom poles on the top and bottom of the icosahedra, which form five intraicosahedral bonds and one intericosahedral bond B(2)-B(2). Note that one of B(1) or B(2) will be a carbon atom in the case of $B_{11}C$ icosahedra. Some work indicates that the carbon atom is located preferentially in a polar B(2) position.[26] The hybridization of the boron and carbon atoms in the icosahedra is unclear, and therefore its contribution to the photoabsorption spectra is similarly uncertain. This will be discussed in the following section.

The atoms in the extreme of the linear chain, either carbon—labeled C(4)—or boron—labeled B(4)—have a tetrahedral-like coordination to three B(1) atoms in three different icosahedra (with a bond length of 1.61 Å) and to the central atom in the chain (with a bond length of 1.43 Å).[27] The hybridization of these C(4) or B(4) atoms should be sp^3-like, and in principle one would expect a near-edge x-ray-absorption fine-structure (NEXAFS) signal resembling that of diamond for C(4) or cubic boron nitride for B(4). The central atom in the chain, labeled B(3), is bonded linearly to the extreme atoms. The hybridization of the central carbon atom is unknown, although some authors propose an sp^2-like hybridization, based on the bond length.[22]

In summary, near the B_4C stoichiometry the structure is supposed to be $B_{11}C$-CBC. That means that there is a carbon atom forming the $B_{11}C$ cluster with an unknown hybridization and two carbon atoms with an sp^3-like hybridization at the extrema of the linear chain. There are 11 boron atoms forming the icosahedron and one boron atom in the center of the linear chain, presumably with an sp^2-like hybridization.

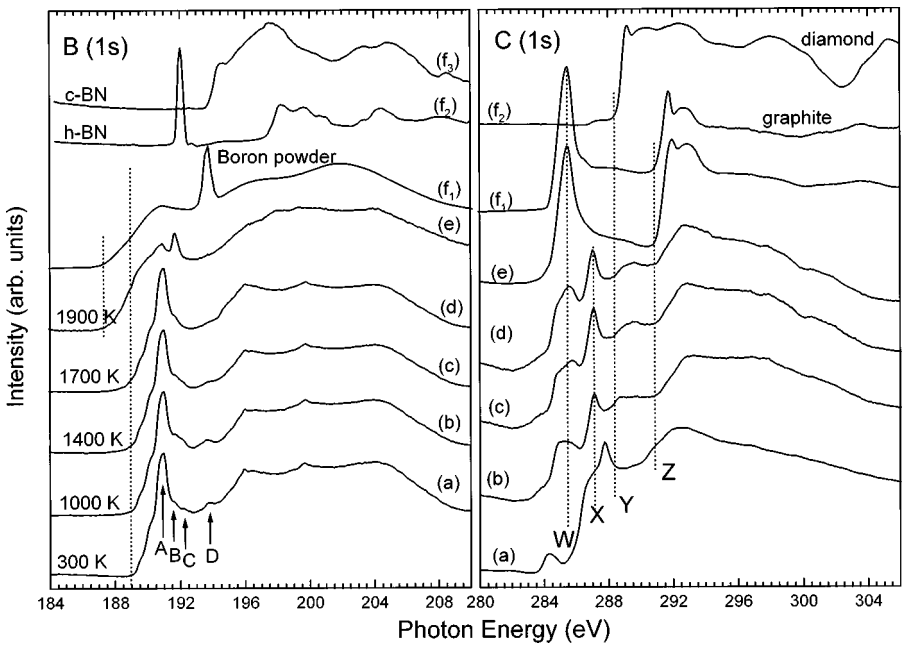

FIG. 2. B(1*s*) and C(1*s*) photoabsorption spectra of boron carbide and reference boron, *h*-BN, *c*-BN, graphite, and diamond samples. Curves (a) correspond to the untreated B_4C sample. Curves (b)–(e) were measured after heating in vacuum to 1000, 1400, 1700, and 1900 K. Curves (f) were obtained from reference samples as indicated in the figure.

IV. RESULTS AND DISCUSSION

A. Photoabsorption: Reference compounds

A simple method of examining the types of bonding present in a solid is based on a direct comparison of x-ray-absorption spectra with reference compounds. This works well to distinguish sp^2 from sp^3 configurations in B, C, and N using as references graphite, diamond, *h*-BN, and *c*-BN. However, the spectra of boron-rich solids based on boron icosahedra are more difficult to be interpreted in such a simple manner, and there is a lack of photoemission and photoabsorption experimental results on these compounds. Previous reports of B_4C photoabsorption spectra disagree in the overall spectral line shape without attempting any interpretation of the results.[28,29] Reference compounds containing boron polyhedra can be the molecular boranes and carboranes.[30,31] In particular, the closo-carboranes are molecules with icosahedral geometry whose unoccupied electronic structure has been studied in detail recently.[32] Previous electronic structure calculations for borane icosahedra with substituted carbon atoms were limited to occupied states.[33]

The type of bonding in the icosahedra must be similar for boron carbide and the closo-carboranes, neither sp^2 nor sp^3. However, one must be aware of the following differences between the carboranes and the solid B_4C. (1) In the closo-carboranes the icosahedron has the $B_{10}C_2$ composition, compared to the $B_{11}C$ icosahedra in boron carbide. (2) Boron carbide is a refractory material with strong bonds among icosahedra, and hence is not a molecular solid (like, e.g., solid C_{60}). It is unclear how much of the molecular orbital structure is retained in the solid. (3) In B_4C there are not only icosahedra, but linear CBC chains as well. Separating the contribution from linear chains and icosahedra to the spectra is an additional problem.

Figure 2 shows a series of boron and carbon photoabsorption spectra from boron carbide and reference carbon, boron, and boron nitride samples. All curves are shown to the same height to illustrate clearly the changes in the spectral shape. Diamond and graphite spectra provide a reference for sp^3 and sp^2 bonding in carbon, and *c*-BN and *h*-BN a reference for sp^3 and sp^2 bonding in boron compounds, respectively. Curves (a) represent the untreated B_4C sample and curves (b)–(e) correspond to the sample annealed with increasing temperatures. The intensities corresponding to the boron carbide spectra along the heating process are displayed in Fig. 3, showing a transition above 1800 K that is discussed below.

B. B(1*s*) photoabsorption

The boron spectra (a)–(d) in Fig. 2 are very similar, indicating that no significant changes in the bonding of boron occur for temperatures under 1700 K. The onset of the ab-

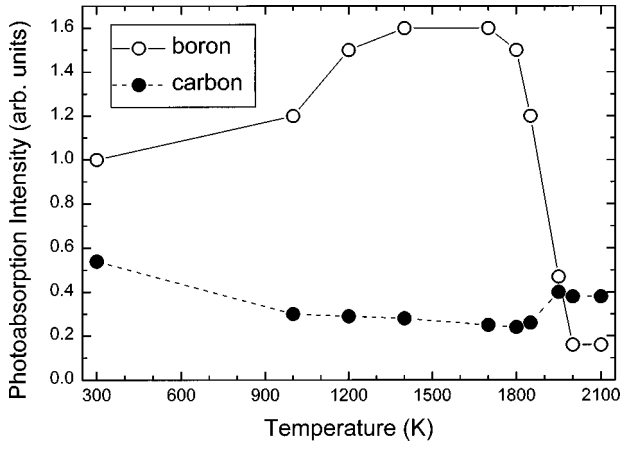

FIG. 3. Development of the B(1*s*) and C(1*s*) photoabsorption intensities with sample heating to increasing temperatures.

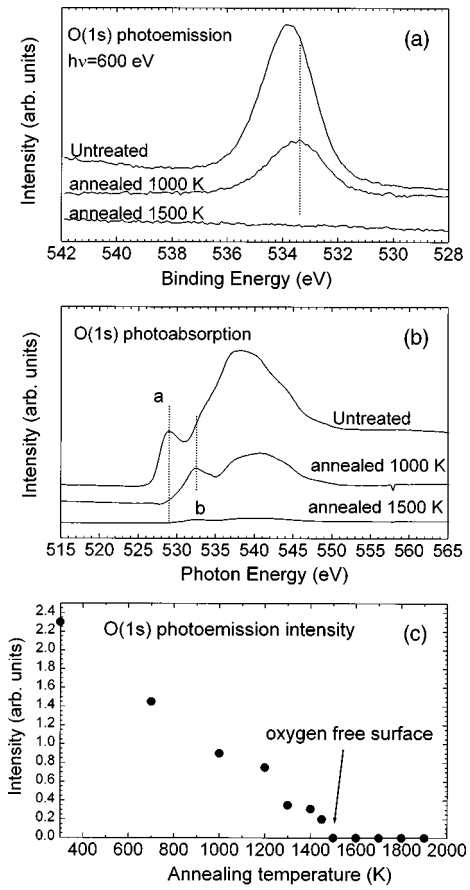

FIG. 4. Oxygen photoemission [panel (a)] and photoabsorption [panel (b)] spectra indicating the presence of oxygen contamination in the untreated sample and the desorption with sample heating in vacuum. Panel (c) represents the photoemission intensity vs heating temperature, evidencing the absence of oxygen at the surface after heating to 1500 K.

sorption occurs at 189 eV, the intensity raising to form an intense peak at 190.9 eV, labeled A, which could be assigned to π^* states from comparison with a similar feature appearing in hexagonal BN at 192.0 eV.[34,35] Three structures appear at about 196, 200, and 204 eV that could be assigned to σ^*-like states from comparison with the BN spectra. Unlike the BN references, the spectra from B_4C do not show separate π^* and σ^* features with well-defined edges. This can be explained by the bonds not being pure π and σ type.

In addition to the main peak at 190.9 eV in Fig. 2, several minor features are present in the 191–194 eV region that change with the annealing temperature. In curve (a) three peaks at 191.7, 192.3, and 193.7 eV labeled B, C, and D are present, feature D being the most intense. In curve (b) peaks B–D are about the same height, and in curve (d) only the peak B at 191.7 is observed. The origin of these features is unclear, except for feature D, which seems related to B_2O_3.[28,29] Photoabsorption and photoemission from the O(1s) core level are shown in Fig. 4 and reveal that a small amount of oxygen is present in the sample which is no longer detected after annealing to 1500 K.

Significant changes in the boron absorption are observed for curve (e), after heating the sample to 1900 K. The onset of absorption is now at 187 eV, peak A, is still present, but is no longer very intense; the prominent feature is now peak B, and the σ^* states have also changed. This evidence reveals the surface instability of boron carbide at 1900 K and indicates that a new phase or a new stoichiometry is attained. These changes can be associated with pure boron as can be seen by comparison to curve (f_1) which represents a reference spectrum obtained from a boron powder. The similarity between curves (e) and (f_1) at the low-energy side of the NEXAFS spectrum is clear, thus suggesting the formation of a boron-rich boron carbide.

According to the above discussion, the typical B(1s) spectrum from an oxygen-free B_4C surface is shown in curve (d) of Fig. 2. This spectrum is similar to the one presented in Ref. 28. The different B_4C spectra shown in Ref. 29 can be explained as a boron-rich boron carbide in their sputter deposited film and to the presence of oxide contamination in their B_4C powder. Comparison of our boron powder spectrum in Fig. 2 with the boron curve in Ref. 28 indicates the presence of oxide in our reference sample by the peak at 193.8 eV. Therefore, the spectrum of clean boron in Ref. 28 is characterized by the lack of any intense and sharp feature. At this point it is interesting to compare our results with the closo-carborane spectra from Ref. 32.

The carborane spectra show an intense peak at $\sim$192 eV which is actually composed of several features in the 191–193 eV range. They correspond to the unoccupied molecular states $10a''$, $17a'$, $26a$, and $27a$ within the lowest excited molecular orbital (LEMO) picture described in Ref. 32. Their character is mostly of p type, with the higher-energy orbitals (LEMO+1,2,...) having more s character than the low-energy one (LEMO). The carboranes also show broad features at 197 and 202 eV of s character. Despite the lack of sharp edges in the carborane spectra, the states with s and p character are separated by a deep valley at 194 eV. The features in the carborane spectra can be associated more directly to the boron and boron carbide spectra when the molecular spectra are shifted $\sim$1 eV to lower energy. The same shift between features in closo-carboranes and B_4C is observed in the C(1s) spectra and is presented and discussed in the next section.

The spectrum of solid boron resembles the carborane spectra widened in such a way that the deep valley is lost. That smooth shape seems characteristic of the boron icosahedra. The spectrum of B_4C, however, contains an intense and sharp peak at 190.9 eV, with a full width at half maximum (FWHM) of 1.1 eV. This peak is sharper than the peak at 192 eV of the carborane molecules, with a FWHM of 2.0 eV for the ortho and 1.7 eV for the meta and para compounds. In general, the spectral features in the gas phase are much sharper than in the solid state, therefore suggesting a distinct origin of the narrower peak in B_4C. The B_4C peak must be related to intericosahedral bonds in the solid. Since that intense feature is not present in solid boron, it should correspond to the bonding between boron icosahedra and the extreme carbon atom in the CBC chain or to bonding within the CBC chain. Another observation of the onset of photoabsorption, which is located at 187 eV for the boron-rich samples and 189 eV in B_4C, should be noted. This shift of 2 eV must correspond to the presence of a carbon atom in the icosahedra in the carbon-rich material.

C. C(1*s*) photoabsorption

The carbon photoabsorption spectra measured on the same sample reveal complementary structural information. Carbon spectra in Fig. 2 correspond to the same stage of the annealing process as the boron spectra with the same label. Curve (e), the one representing the sample heated at 1900 K, looks identical to the graphite reference displayed in curve (f_1), but this structure is not seen in curves (a)–(d). Therefore, the changes occurring at 1900 K are due to segregation of carbon atoms from B_4C to the surface, with the formation of a graphite overlayer. The sample was heated under UHV conditions, thereby precluding carbon contamination from the chamber. The boron carbide in the subsurface region below the graphite layer is boron rich, as evidenced by the B(1*s*) absorption spectra (e), and this is consistent with the carbon segregation. The identification of the graphite as the outer layer is deduced from the strong attenuation of the boron absorption signal after annealing the sample to temperatures above 1800 K as shown in Fig. 3.

The carbon photoabsorption spectrum of B_4C before carbon segregation is dominated by a double feature at 286.7 and 287.7 eV in spectrum (a) that disappears with the sample heating to 1000 K shown in curve (b). This double feature in the C(1*s*) NEXAFS has its counterpart in the O(1*s*) signal, shown in Fig. 4, with peaks at 529.5 and 532.5 eV. The carbon and oxygen peaks correspond to C═O π^* resonances, revealing the presence of carbon oxide contaminants containing carbonyl groups.[36,37] The carbon oxide features disappear uniformly in both the C(1*s*) and O(1*s*) spectra after heating the sample to $\sim$700 K. We have observed the same carbon oxide contamination features in many other *ex situ* prepared samples including boron nitride, titanium nitride, graphite, silicon, etc., but they always disappear after gentle annealing. A similar double peak in the C(1*s*) NEXAFS has been reported in several previous studies of carbon systems and identified as carbon nanotubes features,[38] graphite interlayer states,[39] or the σ^* exciton of amorphous carbon.[40] Our assignment of these features to some C═O moiety is commensurate with the O(1*s*) NEXAFS in all the samples studied and consistent with the disappearance of the features in the C(1*s*) and O(1*s*) spectra after sample outgassing.

Representative NEXAFS spectra of C(1*s*) in B_4C are curves (b)–(d) of Fig. 2, which remain similar for annealing temperatures between 1000 and 1700 K except for a small change in the 285 eV region. In this region there is a double peak at 284.9 and 285.6 eV, the latter becoming more intense with further annealing. This double structure seems related to π bonding, since 285.4 is the energy of the π^* resonance in graphite. Apart from that double peak, the spectrum shows a sharp peak at 287.1 eV, and two smooth edges at 288 and 291 eV.

The most significant features in the boron carbide and reference carbon spectra have been labeled $W-Z$ for direct comparison. The graphite π^* resonance, labeled as W, appears at an intermediate energy between the double peak described above. Peak X at 287.1 eV in boron carbide has no counterpart in the reference spectra. The onset of the σ^* states in sp^3-bonded carbon (diamond reference) is labeled as Y and coincides with the boron carbide edge at 288.3 eV. Feature Z is the onset of the σ^* states in sp^2-bonded carbon (graphite) and coincides with the edge of boron carbide at 291 eV. A possible interpretation of the coincidence of features Y in B_4C and diamond and Z in B_4C and graphite could be the presence of carbon atoms in boron carbide retaining sp^2 and sp^3 hybridization. However, one expects a more complex bonding for carbon in the icosahedra than conventional π and σ bonds.

A better explanation is gained by comparison with the C(1*s*) photoabsorption spectra in closo-carboranes.[32] The carborane signal presents an intense and sharp peak at 288 eV, a double feature at 291–292 eV with the increase of the absorption starting at 290 eV with a smooth edge, a broad feature at 294 eV with an apparent edge at 292.5, and a broader feature at $\sim$298 eV. The sharper peak has been assigned to $10a''$ and $17a'$ states, the double feature at 291–292 eV to $3p$ and $4p$ states, and the two last broader peaks have been assigned to σ^* states. Direct comparison with the B_4C spectra is possible if the molecular spectra are shifted 1 eV to lower energy, in which case peak X lines up with the $10a''/17a'$ molecular peak, edge Y coincides with the apparent edge of $3p/4p$ states, and edge Z with the apparent edge of molecular σ^* states. According to this, features X, Y, and Z correspond to carbon atoms within the icosahedra. Therefore, the features at 284–286 eV would be related to the carbon atoms in the linear CBC chain. In principle, one would expect an sp^3-like signal resembling diamond for these atoms, i.e., an edge at about 288 eV. However, charge transference from carbon to boron atoms and other effects like core hole screening may account for the energy difference of about 3.5 eV. If this is the case, photoemission results should exhibit a similar energy shift for carbon atoms with an sp^3 hybridization in B_4C.

The observed 1 eV shift between the C(1*s*) and B(1*s*) spectra of gas phase closo-carboranes and solid B_4C seems related to a charge effect, since the icosahedra in boron carbide have a composition $B_{11}C$ with an additional electropositive boron compared to $B_{10}C_2$ in closo-carboranes. A gas versus solid state energy shift may also exist, although one expects this effect to be rather small as observed, e.g., in the C(1*s*) photoabsorption π^* resonance from gas benzene versus solid benzene or graphite.[36] A comparison of core level photoemission spectra from boron carbide and closo-carboranes should shed light on this issue.

D. Photoemission

Complementary information about the bonding in B_4C before and after annealing to 1800 K is derived from photoemission spectra. Figure 5 shows a series of C(1*s*) and B(1*s*) core level and valence band photoemission spectra corresponding to another vacuum annealing experiment. The photoemission and photoabsorption measurements were performed in separate experiments using the same set of samples and the temperature being controlled with the same pyrometer.

The C(1*s*) photoemission spectra exhibit large changes during the annealing process. Since only at 1500 K do we stop detecting the oxygen signal, curves (a) and (b) can reveal some type of carbon surface contamination. Curve (c) is a representative spectrum for B_4C, presenting two peaks at

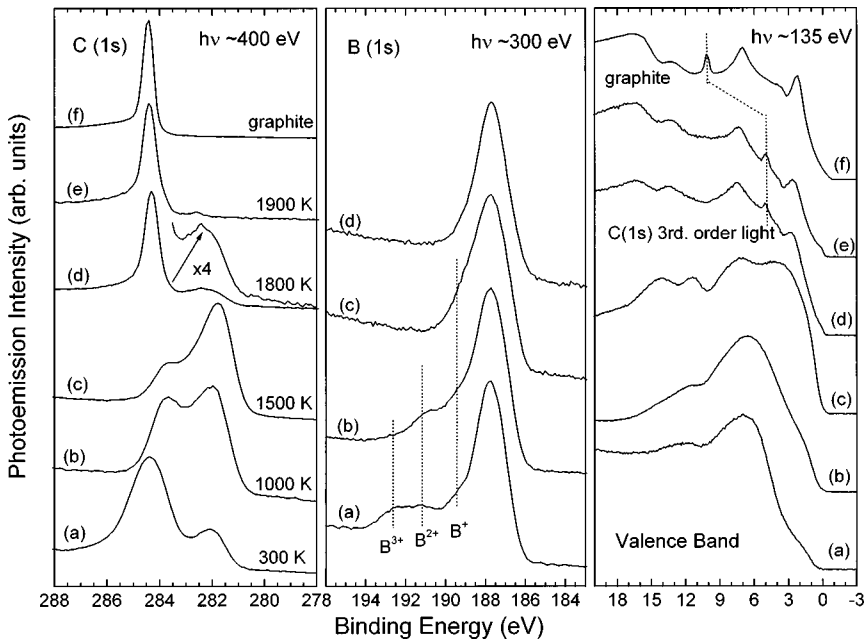

FIG. 5. B($1s$), C($1s$), and valence band photoemission spectra from B_4C. Curve (a) represents the untreated sample, curves (b)–(e) correspond to different annealing temperatures, and curves (f) represent a graphite reference.

281.8 and 283.7 eV. For temperatures over 1800 K a graphite peak at 284.5 eV dominates the spectrum (d), although the overlayer is still thin enough to detect the features at lower binding energy associated with subsurface B_4C. In curve (e), corresponding to annealing to 1900 K, only the graphite peak is present.

The position of the two carbon peaks in spectrum (c) is somehow striking, since both of them have a lower binding energy than the reference graphite. In principle, one would expect a peak corresponding to sp^3 hybridization at a higher binding energy than the graphite reference, since the C($1s$) level in diamond has a higher binding energy than in graphite. A chemical shift of about 0.8 eV has been observed between sp^2 and sp^3 phases in samples containing a mixture of both carbon configurations,[41,42] including the 2×1 surface reconstruction of diamond (111), which presents π bonding.[14] Of course, the binding energy of the core level depends on many factors including the position of the Fermi level within the band gap, charge transfer, and core hole relaxation effects. In the case of boron carbide, the bonds are no longer nonpolar as in graphite and diamond, and charge transfer may affect strongly the binding energy of the core level independently of the sp^2 or sp^3 hybridization of the atoms. Taking into account the structural model for B_4C, one can explain the intensity of the peak at 281.8 eV being double than that of peak at 283.7 by assigning the low-binding-energy feature to the two carbon atoms in the CBC chain and the high-binding-energy one to the carbon atom in the icosahedron. Following this argument, electrons in the sp^3-like carbon atoms of the CBC chain have a binding energy 3.5 eV lower than sp^3 carbon atoms in carbon. This is consistent with the assignment of the C($1s$) photoabsorption features described above.

The B($1s$) core level spectra show the desorption of different oxides with increasing heating temperature. For the untreated sample in curve (a), three different oxide peaks corresponding to oxidation numbers $3+$, $2+$, and $1+$ are present. Curve fitting the spectrum (a) with four component curves yields chemical shift values of 4.9, 3.4, and 1.7 eV, respectively, for the oxides. The FWHM of the B($1s$) core level is 1.7 eV, much broader than the features in the photoabsorption spectrum which are about 0.5 eV FWHM for the π^* features. With annealing the oxides are desorbed, the higher oxidation numbers first, until neither boron oxides nor O($1s$) is detected over 1500 K. For annealing at 1900 K no boron signal is detected due to the thick graphite overlayer.

The valence band spectra are also consistent with the described scenario. Curve (a) shows three broad peaks at about 2, 7, and 12 eV. Curve (b) shows similar features, with a higher intensity of the feature near the valence band maximum as can be expected from boron carbide covered with oxides that are being desorbed. Curve (c) shows new features and a sharper onset at the valence band maximum. Consistently with the previous discussion, we consider this spectrum as typical of the B_4C compound. This valence band spectrum looks similar to previous reports of boron carbide grown from deposition of diethylcarborane on Si(111) and subsequent annealing.[43] The valence band spectra (d) and (e) are identical to the valence band of the graphite reference, as expected from the formation of the graphite overlayer. Note the presence in the spectra of the C($1s$) core level excited from third-order light, a feature that moves in the spectrum with a slight variation of the energy of the incident photons.

V. CONCLUSIONS

In summary, we have performed a photoemission and photoabsorption study of boron carbide to identify the spectral features of this compound of potential interest in many areas of basic and applied surface research, for which hitherto unclear and unconsistent spectra appeared in the literature. We have attempted to relate the spectral features with the bonding environments in B_4C, based on a comparison with reference compounds. Additional theoretical work is re-

quired for a more complete interpretation of the NEXAFS results, which contain much information on the atomic and electronic structure of materials.

This qualitative analysis indicates that many of the features in the boron carbide NEXAFS spectra can be directly related to those of the icosahedral closo-carborane molecules, noting that the molecular spectra are shifted by about 1 eV to higher energies compared to the spectra from the solid. The additional structure in the boron carbide spectra seems related to the linear CBC chains. The onset of absorption from the B($1s$) level shifts 2 eV depending on the icosahedra containing or not a carbon atom. Our results suggest that the carbon atoms in the CBC chain, presumably with sp^3 hybridization, show a binding energy for the $1s$ electrons $\sim$3.5 eV lower than diamond, the prototype solid with sp^3 bonding.

We have performed also a study of the spectral changes observed during annealing, in order to understand surface cleaning procedures and the thermal stability of this compound. We conclude that annealing between 1500 and 1700 K is required to attain a clean surface, and that heating over 1700 K results in carbon segregation to the surface with the formation of a graphite overlayer, leaving a boron-rich boron carbide beneath the graphitic surface.

ACKNOWLEDGMENTS

This work has been supported by the Division of Materials Sciences, Office of Basic Energy Science, and performed under the auspices of the U.S. Department of Energy by Lawrence Livermore National Laboratory under Contract No. W-7405-ENG-48 and the NSF under Contract No. DMR-9632527. The work was performed at the Stanford Synchrotron Radiation Laboratory, which is supported by the Department of Energy, Office of Basic Energy Sciences, and at the Advanced Light Source, LBNL, under Contract No. DE-AC03-76SF00098. I.J. acknowledges financial support from the Spanish CICYT project PB94-53 and NATO project CRG-971539.

*Present address: Instituto de Ciencia de Materiales de Madrid (CSIC), Cantoblanco, E-28049, Spain. Electronic address: ijimenez@icmm.csic.es

[1] D. Emin, Phys. Today **40**(1), 55 (1987).
[2] G. H. Kwei and B. Morosin, J. Phys. Chem. **100**, 8031 (1996).
[3] A. J. Pyzik and D. R. Beaman, J. Am. Ceram. Soc. **78**, 305 (1995).
[4] L. L. Wang, Z. A. Munir, and J. B. Holt, J. Am. Ceram. Soc. **78**, 756 (1995).
[5] L. S. Sigl and H. J. Kleebe, J. Am. Ceram. Soc. **78**, 2374 (1995).
[6] S. Lee, J. Mazurowski, G. Ramseyer, and P. A. Dowben, J. Appl. Phys. **72**, 4925 (1992).
[7] S. Lee and P. A. Dowben, Appl. Phys. A: Solids Surf. **58**, 223 (1994).
[8] H. Wehrheit, in *The Physics and Chemistry of Carbides, Nitrides and Borides*, edited by R. Freer (Kluwer, Amsterdam, 1990), p. 677.
[9] D. Emin, in *The Physics and Chemistry of Carbides, Nitrides and Borides* (Kluwer, Amsterdam, 1990), p. 691.
[10] R. Riedel, A. Kienzle, W. Dressler, L. Ruwisch, J. Bill, and R. Aldinger, Nature (London) **382**, 796 (1996).
[11] J. von Seggern, V. Philipps, P. Wienhold, A. Pospieszczyk, H. G. Esser, and J. Winter, Vacuum **47**, 935 (1996); P. Sonato *et al.*, *ibid.* **47**, 977 (1996).
[12] K. N. Kushita, K. Hojou, and S. Furuno, Microsc. Microanal. Microstruct. **6**, 149 (1995).
[13] R. Jimbou, N. Ogiwara, M. Saidoh, K. Morita, K. Mori, and B. Tsuchiya, J. Nucl. Mater. **220/222**, 869 (1995).
[14] J. F. Morar, F. J. Himpsel, G. Hollinger, J. L. Jordan, G. Hughes, and F. R. McFeely, Phys. Rev. B **33**, 1340 (1986).
[15] L. J. Huang, I. Bello, W. M. Lau, S. T. Lee, P. A. Stevens, and B. D. DeVries, J. Appl. Phys. **76**, 7483 (1994).
[16] F. J. Himpsel, J. F. van der Veen, and D. E. Eastman, Phys. Rev. B **22**, 1967 (1980).
[17] N. J. Wu and A. Ignatiev, Phys. Rev. B **25**, 2983 (1982).
[18] D. J. G. Sutherland, H. Akatsu, M. Copel, F. J. Himpsel, T. A. Callcot, J. A. Carlisle, D. L. Ederer, J. J. Jia, I. Jimenez, R. Perera, D. K. Shuh, L. J. Terminello, and W. M. Tong, J. Appl. Phys. **78**, 6761 (1995).
[19] H. K. Clark, and J. L. Hoard, J. Am. Chem. Soc. **65**, 2115 (1943).
[20] D. R. Tallant, T. L. Aselage, and D. Emin, in *Boron-rich Solids*, edited by D. Emin, T. L. Aselange, A. C. Switendick, B. Morosin, and C. L. Beckel, AIP Conf. Proc. No. 231 (AIP, New York, 1991), 177 ; H. Stein, T. Aselage, and D. Emin, *ibid.*, p. 322.
[21] U. Kuhlmann and H. Werheit, Phys. Status Solidi B **175**, 85 (1993).
[22] J. Conard, M. Bouchacourt, F. Thevenot, and G. Hermann, J. Less-Common Met. **117**, 51 (1986).
[23] E. L. Venturini, L. J. Azevedo, D. Emin, and C. Wood, in *Boron-rich Solids*, edited by D. Emin, T. L. Aselange, C. L. Beckel, I. A. Howard, and C. Wood, AIP Conf. Proc. No. 140 (AIP, New York, 1986), p. 292.
[24] D. Emin, Phys. Rev. B **38**, 6041 (1988).
[25] U. Kuhlmann and H. Wehrheit, Solid State Commun. **83**, 849 (1992).
[26] H. Werheit, U. Kuhlmann, and T. Lundström, J. Alloys Compd. **204**, 197 (1994).
[27] T. L. Aselange and D. Emin, in *Boron-rich Solids*, edited by D. Emin, T. L. Aselange, A. C. Switendick, B. Morosin, and C. L. Beckel, AIP Conf. Proc. No. 231 (AIP, New York, 1991), p. 177.
[28] D. Li, G. M. Bancroft, and M. E. Fleet, J. Electron Spectrosc. Relat. Phenom. **79**, 71 (1996).
[29] J. J. Jia, J. H. Underwood, E. M. Gullikson, T. A. Callcott, and R. C. C. Perera, J. Electron Spectrosc. Relat. Phenom. **80**, 509 (1996).
[30] S. Lee, P. A. Dowben, A. T. Wen, A. P. Hitchcock, J. A. Glass, and J. T. Spencer, J. Vac. Sci. Technol. A **10**, 881 (1992).
[31] A. P. Hitchcock, A. T. Wen, S. Lee, J. A. Glass, J. T. Spencer, and P. A. Dowben, J. Phys. Chem. **97**, 8171 (1993).
[32] A. P. Hitchcock, S. G. Urquhart, A. T. Wen, A. L. D. Kilcoyne, T. Tyliszczak, E. Rühl, N. Kosugi, J. D. Bozek, J. T. Spencer, D. N. McIlroy, and P. A. Dowben, J. Phys. Chem. B **101**, 3483 (1997).
[33] T. A. Green, A. C. Switendick, and D. Emin, J. Chem. Phys. **89**, 6815 (1988).
[34] I. Jiménez, A. Jankowski, L. J. Terminello, J. A. Carlisle, D. G. J.

Sutherland, G. L. Doll, J. V. Mantese, W. M. Tong, D. K. Shuh, and F. J. Himpsel, Appl. Phys. Lett. **68**, 2816 (1996).
[35] I. Jiménez, A. Jankowski, L. J. Terminello, D. G. J. Sutherland, J. A. Carlisle, G. L. Doll, W. M. Tong, D. K. Shuh, and F. J. Himpsel, Phys. Rev. B **55**, 12 025 (1997).
[36] J. Stöhr, *NEXAFS Spectroscopy* (Springer, Berlin, 1992).
[37] A. P. Hitchcock and D. C. Mancini, J. Electron Spectrosc. Relat. Phenom. **67**, 1 (1994).
[38] M. Imamura, H. Shimada, N. Matsubayashi, M. Yumura, K. Uchida, S. Oshima, Y. Kuriki, Y. Yoshimura, T. Sato, and A. Nishijima, Jpn. J. Appl. Phys., Part 1 **33**, L1017 (1994).
[39] D. A. Fischer, R. M. Wentzcovitch, R. G. Carr, A. Continenza, and A. J. Freeman, Phys. Rev. B **44**, 1427 (1991).
[40] A. Gutiérrez and M. F. López, Europhys. Lett. **31**, 299 (1995).
[41] J. Díaz, G. Paolicelli, S. Ferrer, and F. Comin, Phys. Rev. B **54**, 8064 (1996).
[42] J. Schäfer, J. Ristein, R. Graupner, L. Ley, U. Stephan, Th. Frauenheim, V. S. Veerasamy, G. A. J. Amaratunga, M. Weiler, and H. Ehrhardt, Phys. Rev. B **53**, 7762 (1996).
[43] F. J. Perkins, M. Onellion, S. Lee, D. Li, J. Mazurowski, and P. A. Dowben, Appl. Phys. A: Solids Surf. **54**, 442 (1992).